JCTC Journal of Chemical Theory and Computation

Theoretical DFT Study on the Interaction of NO and Br_2 with the Pt(111) Surface

Nurbosyn U. Zhanpeisov* and Hiroshi Fukumura

Department of Chemistry, Graduate School of Science, Tohoku University, Sendai 980-8578, Japan

Received December 7, 2005

Abstract: Density functional calculations were performed at the B3LYP level using combined basis sets for the NO and bromine interactions with the Pt(111) surface mimicked by the two-layer Pt_{10} cluster model. It explains well an attractive bonding interaction not only for bromine and Pt(111) but also for all three adsorption modes of NO on the Pt(111) surface. In accordance with the experimental observations, the calculations predict that the first peak in the IR spectra appears at around 1515 cm^{-1} at the initial stage of low NO coverage, while it would shift to 1707 cm^{-1} at high NO coverage. The bonding of NO on the 3-fold hollow fcc and hcp sites of Pt(111) proceeds via predominant back-donation interactions, while for the on-top adsorption, both the donation and back-donation interactions become equally important. Energetic criteria show also that the STM tip (made from Pt and Ir alloys) immersed into a bromine solution may contain only dissociated bromine atoms that bind strongly with the surface Pt atoms. As a result, the ν_{BrBr} stretching vibration mode for the bromine molecule may not be seen in the IR spectra because of its dissociation into adsorbed atoms. This leads to an appearance of a blue shifted band centered at ca. 202 cm^{-1}.

Introduction

Interaction of NO with metal surfaces and, in particular, with Pt and Pd has been the subject of many experimental and theoretical investigations because of considerable interest in the field of heterogeneous catalysis and various catalytic processes.[1−12] One of the important examples is a reduction of toxic NO_x from flue gases emitted by stationary and mobile sources, automobiles, coal-fired power plants, electric power generators, nitric acid factories, etc.[6,13,14] Since NO_x are the most toxic environmental pollutants, the control of NO emissions is a major challenge and the most highly desirable goal. Despite general agreement on a molecularly adsorption feature of NO on a Pt surface at low temperatures, there are still controversial discussions on the nature of target interactions and stable adsorption sites on the Pt(111) surface. Recently, Nakatsuji et al.[6] have shown that only the dipped admolecule model (DAM) can properly describe both the energetics and the vibrational modes for the NO adsorbed on the Pt(111) surface, while they have ruled out the adequacy in applying the so-called cluster model approach to mimic such kinds of interactions. At the same time, Trout et al.[7] have claimed that the periodic slab calculations can be also well suited in describing these interactions including such features as the order of stability for the adsorption complexes and their adsorption energies when considering the different adsorption modes realized on Pt(111). However, these latter two quantities, i.e., the relative stability order and adsorption energies, differ strongly from those predicted by Nakatsuji et al.[6]

Another aspect related to the Pt surface is studies on the adsorption of bromine or iodine species at different Pt facets that has been widely investigated under ultrahigh vacuum, at normal atmospheric pressure conditions as well as from aqueous solutions.[15−18] At temperatures as low as 25 K, bromine is dissociatively adsorbed on Pt(111). The strong interaction between bromine radicals and the Pt surface accounts for Br_2 dissociative adsorption. These adsorbed bromine atoms are supposed to be only transiently mobile,

* Corresponding author phone: 81-22-795-6568; e-mail: nurbosyn@orgphys.chem.tohoku.ac.jp.

10.1021/ct050308m CCC: $33.50
Published on Web 04/07/2006

while weakly bound Br_2 molecules would be adsorbed near or preexisting Br atoms that would act as preferential sites for Br_2 dissociation. Under atmospheric pressure conditions, the exposure of clean Pt(111) surface to bromine vapors results in the formation of about half of the monolayer coverage of bromine atoms while being neutral in character for the adsorbed bromine atoms. Earlier Solomon et al.[19] studied iodine molecule adsorption on steps of the Pt surface under vacuum and atmospheric pressure conditions using experimental LEED, AES, and thermal desorption spectroscopies. In contrast to smooth Pt(111), they found multiple phase domains of (3×3) or $(\sqrt{3}\times\sqrt{3})\times R30°$ and no special preferences for iodine adsorption on these step positions. Ertl and co-workers[20] have also shown that bromine adlayers formed by flame annealing of platinum single-crystal surfaces and quenching in bromine vapor, studied by STM and cyclovoltammetry, form protective layers which, similar to iodine, prevent contamination of the surface and lead to well-defined surfaces. On Pt(111), a (4×4) structure is observed, while on Pt(100), a disordered structure is observed. Both structures are compatible with densely packed adlayers of bromine, while all three low index surfaces including Pt-(110) yield air-stable bromine adlayers.

Since the discovery of powerful STM techniques in 1982,[21] to attain their main goals, scientists are driven not only to understand how atoms locate at surface interfaces and how they behave with the surface electrons but also to understand deeply the STM tip enhanced spectroscopic properties of adsorbed molecules and highly ordered structures as well as polymerization processes on different substrates.[22−24] Using this technique one may effectively initiate chemical reactions of interest, manipulate the oxidation or reduction processes at distinct active surface sites, etc. This methodology is also important in creating new microchips for optoelectronic devices, computers, etc. Also, because of considerable interest in the modification of STM tips through contacts with bromine or iodine solutions, theoretical considerations may further supplement a deep understanding of those unique properties at target surfaces and their interfaces. Moreover, they can be expected to be equally complimentary for the experimental investigations. The question that arises as to what extent this halogen modification of the STM tip can lead is of primary interest because the tip enhanced IR or Raman spectra is the origin to obtain additional information not only on surface structures but also on the quality of surfaces as well as on their environment.

In this paper, we report on the theoretical results obtained for the interaction of the NO and bromine with Pt(111) using the cluster approach. In contrast to the cited above most recent publications,[6,7] we will show that the cluster approach can be equally applied to describe reasonably the nature of the target interactions as well as to predict theoretical spectroscopic properties of adsorbed molecules. In particular, the IR spectra of NO acted as a probe molecule, and bromine on Pt(111) can be well explained.

Method and Models

Density functional theory (DFT) calculations were performed using the Gaussian03 program packages.[25] Geometry optimizations were carried out with the use of Becke's three-parameter hybrid method with the Lee, Yang, and Parr (B3LYP) gradient-corrected correlation functional[26] and the combined standard basis sets. The latter basis sets include the standard 6-31G* ones for the N and O atoms and Lanl2dz basis sets for all the Pt as well as Br atoms. As a result, they would be denoted as the B3LYP/(Lanl2dz + 6-31G*) level for the NO on the Pt(111) and B3LYP/Lanl2dz level for bromine on Pt(111), respectively. The Pt(111) surface was modeled by the two-layer Pt_{10} cluster model shown in Figure 1. The geometry optimizations were carried out taking into account symmetry restrictions and followed by estimation of vibration fundamentals via performing harmonic frequency calculations.

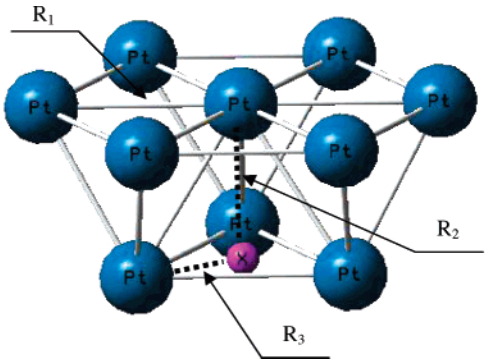

Figure 1. The two-layer Pt_{10} cluster model mimicking the Pt-(111) surface and the definition of the three independent variables.

Results and Discussion

The ground electronic state of the isolated Pt atom is $^3D_3$ with the electronic configuration of [Xe]: $4f^{14}5d^96s^1$. Because of this triplet ground state, it is not evident how the overall spin state would be for the cluster consisting of 10 Pt atoms. Trout et al.[7] have excluded in their calculations magnetic states and have performed only nonmagnetic slab calculations for the combined systems of the NO adsorbed on Pt because the chemisorbed NO is found to be nonspin-polarized according to previous studies.[2] However, this is not necessarily true either for the isolated Pt cluster with a finite size or for the combined adsorption complexes of NO considered here. To clarify this issue, we have first determined the optimal spin state for the isolated two-layer Pt_{10} cluster model. Table 1 lists the results of these calculations. Note that for each spin state the three independent structural parameters shown in Figure 1 were optimized. As is clear the closed-shell singlet spin state is highly unfavorable for the Pt_{10} cluster by energy (about 30 kcal/mol) than the optimal spin state one containing eight unpaired electrons with a multiplicity equal to 9. The spin densities for these 8 electrons are distributed over all the Pt atoms while being less localized on the central Pt site. Its spin equals only to 0.276. In addition, this state is free from spin contaminants because its $/S^2/$ value after spin annihilation matches exactly with the theoretical value of 20.

Moreover, the central Pt atom is the only site with a positive charge of $0.274e^-$ after conventional Mulliken population analysis, while the rest of the other Pt atoms in

Table 1. Multiplicity (M), Relative Energy (E_{rel}, kcal/mol), Value of $/S^2/$ before (after) Spin Annihilation, and Geometry (R_1, R_2, R_3, All in Å) of the Bare Pt_{10} Cluster

M	E_{rel}[a]	$/S^2/$	R_1	R_2	R_3
1	29.7		2.707	2.201	1.621
3	7.3	4.03 (5.44)	2.709	2.218	1.645
5	5.0	7.03 (6.35)	2.712	2.218	1.641
7	1.7	12.51 (12.04)	2.725	2.187	1.623
9	0	20.10 (20.00)	2.720	2.203	1.682
11	14.7	30.10 (30.00)	2.723	2.205	1.688

[a] Total energy of the bare cluster with multiplicity equal to nine is taken as an internal reference. The positive sign corresponds to lower stability.

the cluster are all slightly negatively charged. Evidently, the obtained high-spin state for the Pt_{10} cluster should be taken into account when considering the adsorption complexes of NO and bromine because they would strongly affect their adsorption energetics.

Thus, we have first examined the adsorption complexes of the NO molecule on the Pt_{10} cluster. Because the isolated NO molecule has one unpaired electron in its π^*-MO and radical in nature, the interaction with the high-spin Pt_{10} cluster leads to effectively coupling of these electrons. Therefore, the bonding between the NO and the Pt_{10} cluster can be governed by the donation and/or back-donation interactions. Nakatsuji et al.[6] have pointed out that for this target interaction the back-donation is more important and dominant and that the interaction can be only explained within the DAM model, while the cluster approach will fail to explain this bonding phenomenon. However, here we have some doubt about this conclusion. Below we will show that both donation and back-donation interactions are equally important and depend on the distinct adsorption modes. Moreover, the cluster model can be also considered as a complementary tool to reliably explain both the energetics of the NO adsorption and spectroscopic properties of the adsorbed NO on Pt(111).

Table 2 lists the adsorption energies, molecular properties, and main geometric parameters for the NO adsorption at the most common three active sites of Pt(111) mimicked by the Pt_{10} cluster model, while the stick and ball optimized geometries of adsorption complexes are shown in Figure 2. These adsorption modes correspond to the bonding of NO on the top site as well as on both the 3-fold hollow fcc and hcp sites. The latter two sites differ only by the absence or presence of the Pt atom of the second layer just below the center of the top 3-fold hollow site. Note that this applied Pt_{10} cluster model is the minimal one that contains all the sets of active sites on Pt(111). However, one should keep in mind that the use of such a kind of finite cluster model has well-documented disadvantages in describing extended surfaces.[10] Nevertheless, the applied Pt_{10} cluster model is well suited to the broad survey undertaken here, being computationally much less demanding than those based on the periodic slab approach.

As in the case of the isolated cluster model, for each adsorption mode considered here we have selectively determined the optimal spin state for the combined system. Accordingly, the optimal spin state for each adsorption complex together with their $/S^2/$ values are shown in Table 2. An analysis of these data shows the following peculiarities:

(i) The applied cluster model can explain the attractive bonding interaction between the NO and the Pt(111) surface

Table 2. Adsorption Energy (E_{ads}, kcal/mol), Multiplicity (M), Value of $/S^2/$ before (after) Spin Annihilation, Charges (Q_{NO} and Q_{Pt}, e^-) on NO and the Central Pt Atom, Spin Density (ρ_{NO}, e^-) on NO, Bond Lengths (R_{Pt-N} and R_{N-O}, Å), NO Stretching Frequency (ν, cm^{-1}), and HOMO and HOMO−LUMO Gap (Δ, au) for the Adsorption Complexes of NO on Pt(111) Mimicked by the Two-Layer Pt_{10} Cluster Model as Calculated at the B3LYP/(Lanl2dz + 6-31G*) Level

	on-top	fcc	hcp
E_{ads}[a]	19.1	14.8	14.1
	18.2	14.2	13.6
	19.3	16.8	16.1
M	8	6	6
$/S^2/$	15.82 (15.75)	8.92 (8.76)	8.86 (8.75)
Q_{NO}	+0.03	−0.46	−0.44
Q_{Pt}	−0.14	+0.16	+0.18
ρ_{NO}	+0.07	−0.06	−0.07
R_{Pt-N}	2.052	2.104 (1.999)[b]	2.104 (2.001)[b]
R_{N-O}[c]	1.167	1.205	1.204
ν_{NO}[d]	1707	1515	1530
HOMO	−0.2073	−0.2059	−0.2049
Δ	0.0654	0.0530	0.0585

[a] The values of adsorption energies at the second and third rows were estimated at the B3LYP/(Lanl2dz + 6-311++G**)//B3LYP/(Lanl2dz + 6-31G*) and B3LYP/(Lanl2dz + cc-pVTZ)//B3LYP/(Lanl2dz + 6-31G*) levels of theory, respectively. [b] The other two equal Pt−N bond distances formed by the N atom and the two nearest edge Pt atoms are shown in parentheses. [c] The N−O bond distance in the gas phase is calculated to be equal to 1.159 Å. [d] The ν_{NO} stretching frequency is scaled down by using a scale factor of 0.97.[30]

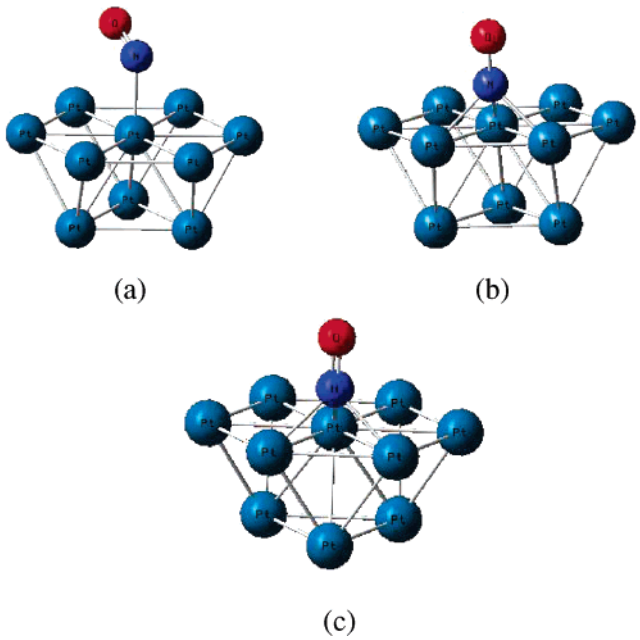

Figure 2. The optimized adsorption complexes of NO on the Pt(111) surface presented in stick and ball structures: (a) on-top, (b) 3-fold hollow fcc, and (c) 3-fold hollow hcp adsorption complexes.

for all three adsorption modes. This finding is in contrast with the conclusions of ref 6, where highly repulsive interactions have been observed for all the adsorption modes of NO on a similar Pt_{10} cluster model. For example, the adsorption of NO on the on-top, 3-fold hollow fcc and hcp sites was found to be highly unstable for 32.5, 35.3, and 36.9 kcal/mol, respectively.[6] Two factors, i.e., basis set inconsistency and low spin state for the Pt_{10} cluster applied, might be the reason for the latter repulsive interactions found in ref 6. Moreover, we have also found that the bonding mechanism is not one and the same for all three adsorption modes. For the on-top adsorption mode, both the donation and back-donation is equally important, with a slight preference only for the donation of the electron density from the NO molecule to the Pt(111) surface. The net electron density transfer amounts to $0.03e^-$. For the other two 3-fold hollow fcc and hcp sites, the back-donation is strictly predominant as can be seen from the Mulliken population analysis (see Table 2). As a result, the latter back-donation lowers the overall spin state for these adsorption modes. However, in accordance with the results of other previous studies,[2,7] the adsorbed NO molecule is nonspin-polarized because of negligibly small spin density on the N and O atoms for all three adsorption complexes.

We have also performed additional calculations for population analysis and atomic charge assignments that are based on natural bond orbital (NBO) analysis and charges determined by the fit to the electrostatic potential at points selected according to the CHelpG scheme.[25] The latter CHelpG charges support qualitatively the above findings; however, they are highly dependent on the radii of the centers used in fitting those potentials. NBO analysis shows that the d-population on the central Pt atom is smaller for ca. 0.10 e^-, while its 6p-AO earns ca. $0.13e^-$ as compared to other Pt sites in the case of the on-top adsorption mode of NO. The electronic configurations for the N and O atoms become $[He]2s^{1.64}2p^{3.16}$ and $[He]2s^{1.72}2p^{4.43}$, respectively. Conversely, the adsorption of NO on the 3-fold hollow fcc site decreases the d-population on the three Pt atoms of interest by 0.17, 0.14, and 0.14 e-, while electronic configurations of the N and O atoms look like $[He]2s^{1.44}2p^{3.59}$ and $[He]2s^{1.72}2p^{4.50}$, respectively. As is clear, a strong population of 2p-AO of the N site of NO is observed. A similar picture has been also observed for the adsorption of NO on the 3-fold hollow hcp site. Thus, the back-donation interaction favors the NO binding at high-coordination fcc and hcp sites, while the donation term is consistently more favorable for the on-top coordination.

(ii) The adsorption energies estimated in a conventional way lie in close proximity to each other with a slight preference (about 5 kcal/mol) for the on-top adsorption mode. The least stable mode is the adsorption on the 3-fold hollow hcp site, which is about 0.7 kcal/mol less strong than that of the 3-fold hollow fcc site. Thus, the order of stability is expressed as on-top $>$ fcc $\approx$ hcp and correlates with the highest occupied molecular orbital (HOMO) level. Additional single-point calculations were performed at the same B3LYP level, but using more larger and extended basis sets did not alter the above obtained stability order (see the second and third rows for the adsorption energy, Table 2). Also, the adsorption energies estimated at the B3LYP/(Lanl2dz + 6-31G*) level lie within 1−2 kcal/mol as compared to those estimated at higher levels of the theory for each selected adsorption mode of the NO on Pt(111). However, this obtained stability order of adsorption complexes is in contrast with the results of other theoretical studies[6,7] but supports well the results of an experimental study obtained by Matsumoto et al.[27] According to the latter experimental interpretation, NO occupies the three sites sequentially depending on the NO coverage. First NO adsorbs at the 3-fold hollow fcc site, next at the top site, and last at the 3-fold hollow hcp site.

The above findings of ours need additional remarks. A traditional picture proposed by Gland and Sexton[1b] for the interaction of NO with Pt(111) points out that at low coverages bridge sites are initially occupied by NO molecules. This erroneous ascription has been, however, later corrected by other studies[1c,3,27] so that it turned out to be 3-fold hollow fcc sites. Gland and Sexton[1b] claimed also that the bridge NO species leaves the bridge sites and moves to the on-top sites as the NO coverage increases that is based on the disappearance of the vibrational band at 1490 cm^{-1} at high NO coverage in the reflection absorption infrared spectroscopy measurements (RAIRS). However this mode remains in the high-resolution electron energy loss spectroscopy measurements (HREELS) even at the saturation coverage. Therefore, the site transfer model proposed by Sexton and Gland[1b] is insufficient and is not applicable to explain the discrepancy between the results of RAIRS and HREELS. Moreover, the previous theoretical calculations[3,6,7] have shown also that the 3-fold hollow fcc site is the most preferable adsorption site, so that there are no reasons for the move of the adsorption complex from the 3-fold hollow fcc site to on-top sites, at least at coverages lower than 0.25 multilayers. In addition, why the on-top species exists is irrespective of the relative instability as compared to the above 3-fold hollow fcc and hcp site species. The latter picture is even highly pronounced in ref 6, where the relative stability of the adsorption complexes on the 3-fold hollow fcc and the hcp sites are ca. 3.5 times larger than that of the on-top site that even rules out the formation of the latter adsorption complexes. Thus, our results obtained above are in line with the interpretation proposed by Matsumoto et al.,[27] and the move from the 3-fold hollow fcc site to the on-top site is driven by a slight preference in the adsorption energy for the latter on-top sites.

(iii) The adsorption of NO leads to the elongation of the N−O bond length as compared to the isolated gas-phase value. This increase in the bond distance is larger for the adsorption of NO on the 3-fold hollow fcc and hcp sites being about 0.05 Å. Note also that the two latter adsorption complexes of NO on 3-fold hollow sites result in the formation of three nonequivalent Pt−N bonds because of the shift of the center of mass of NO from the center of the respective hollow sites to the nearest edge site. The nearest distance from the metal surface amount to 1.291 and 1.293 Å for the adsorption complexes on the 3-fold hollow fcc and hcp sites, respectively. Note that the most stable on-top

adsorption mode of NO observed in the present study results in the formation of a tilted structure, the tilt angle being equal to 59.5°. This finding is in line with the results of other investigations on the adsorption of NO on Pt(111)[3,6,7] as well as on Pd(111).[28] Also, the geometry parameters that characterize these three adsorption complexes of NO (i.e., the N−O and Pt−N bond distances, see Table 2) are in good agreement with the observed data of the NEXAFS[5] and LEED[29] experiments.

(iv) The stretching frequency of NO shows a red shift during the adsorption as compared to that of the isolated gas-phase value. For the on-top adsorption complex, it appears at 1707 cm^{-1}, while for the 3-fold hollow fcc and hcp sites they are centered at 1515 and 1530 cm^{-1}, respectively. Because the adsorption energies differ slightly as well as these three adsorption sites equally available, we may conclude that at a low NO coverage, the adsorption takes place on 3-fold hollow sites, while the increase in the NO coverage will result on adsorption on the top sites. Accordingly, at the initial stage of a low NO coverage, the first peak would appear at around 1515 cm^{-1}, while it would shift to 1707 cm^{-1} at high NO coverage. These findings are in complete accordance with the observed experimental data (see, for example, ref 6).

Following the symmetry of the Pt_{10} cluster model, we have considered also some representative structures on extended models. The first one is obtained from Pt_{10} by an increase in Pt atoms at the top layer only (the Pt_{22} cluster model containing 19 and 3 atoms in two layers, respectively), while the second cluster corresponds to the Pt_{31} one containing atoms from the next shell in both layers (19 and 12 atoms at each layers, respectively, see Figure 3). Because of the size of these clusters, single point calculations at the similar B3LYP/Lanl2dz level were carried out to estimate an optimal spin state for these two cluster models at fixed geometries found for the Pt_{10} cluster (at its optimal high spin state). It was found that the energetically most preferable states are those containing 16 and 20 unpaired electrons for the Pt_{22} and Pt_{31} cluster models, respectively. The on-top adsorption mode of NO on the Pt_{22} cluster results in close geometrical parameters and adsorption energy as those found for the case of the minimal Pt_{10} cluster model. For example, the Pt−N and N−O bond distances are equal to 2.000 and 1.159 Å, respectively, while its adsorption energy amounts to 24.6 kcal/mol, an increase of 5.5 kcal/mol as compared to that found for the on-top adsorption on the Pt_{10} cluster model.

Let us move to consider the interaction of the bromine with the Pt(111) surface. As we have noted before, this issue is important, at least in relation to the STM tip modification and in understanding the nature of the target interaction. Note that in STM experiments the most common tip is made from a tungsten polycrystalline wire, while others are based on transition metals usually made from Pt and iridium alloys. To the first approximation, one may consider just a very dense Pt(111) structure as the tip and clarify its interaction with the bromine. Based on the above results obtained for NO interactions with the same Pt_{10} cluster model, we have considered adsorption modes for the bromine molecule and the atom on the top position of Pt(111) as well as the dissociative adsorption form of Br_2. Table 3 lists the results of these calculations, while Figure 4 shows their optimized

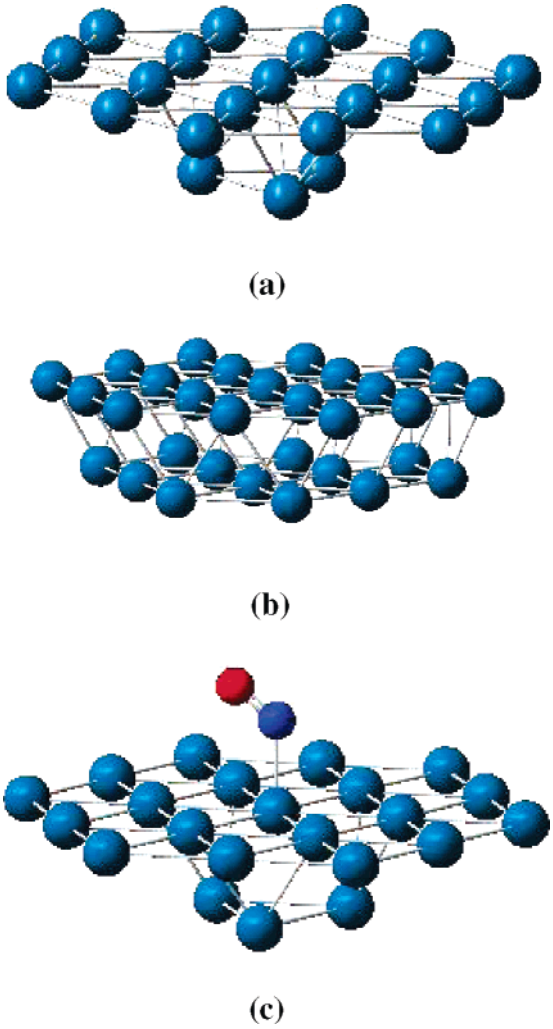

Figure 3. The extended cluster models of Pt_{22} (a) and Pt_{31} (b) as well as the optimized structure mimicking on-top adsorption mode of NO on the Pt_{22} cluster (c).

Table 3. Adsorption Energy (E_{ads}, kcal/mol), Multiplicity (M), Value of $/S^2/$ before (after) Spin Annihilation, Charges (Q_{Br} and Q_{Pt}, e^-) on the Br and Central Pt Atoms, Spin Density (ρ_{Br}, e^-) on the Adsorbate, Bond Lengths (R_{Pt-Br} and R_{Br-Br}, Both in Å), and HOMO (au) for the On-Top Adsorption Complexes of Br_2 and Br as Well as Dissociative Adsorption of Br_2 on Pt(111) Mimicked by the Two-Layer Pt_{10} Cluster Model

	on-top Br_2	on-top Br	dissociative Br_2
E_{ads}	20.4	42.5	72.9
M	9	8	9
$/S^2/$	20.10 (20.00)	15.81 (15.75)	20.07 (20.00)
Q_{Br}	+0.03 (−0.27)[a]	+0.04	+0.05 (+0.04)[b]
Q_{Pt}	+0.08	−0.24	−0.24
ρ_{Br}	+0.02 (+0.03)[a]	+0.03	+0.04 (+0.12)[b]
R_{Pt-Br}	2.720	2.570	2.568 (2.663)[b]
R_{Br-Br}	2.749		
HOMO	−0.2226	−0.2167	−0.2240

[a] The value in parentheses is for the end bromine atom. [b] The value in parentheses is for the Br atom that bonds with the nearest two edge Pt atoms.

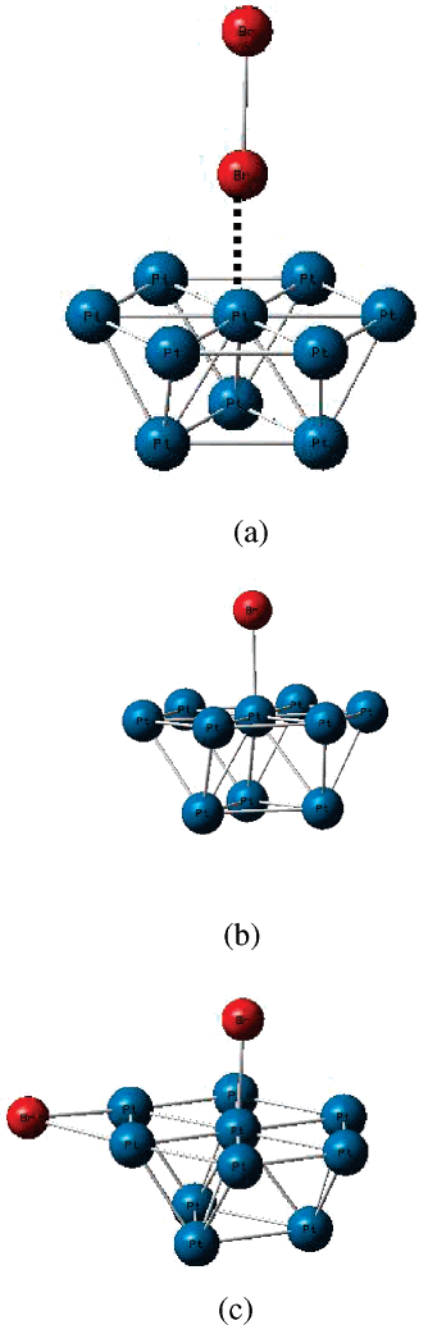

Figure 4. The optimized adsorption complexes of (a) molecular Br_2 and (b) atomic Br on the top position and (c) dissociative adsorption of Br_2 on-top as well as the two edge Pt atoms of the Pt(111) surface.

geometries. An analysis of these data shows that the molecular adsorption of Br_2 on the top position of Pt(111) is twice as weak as that of the atomic Br adsorption. Moreover, the molecular adsorption is much less profitable as compared to its dissociative adsorption form. In the latter dissociative adsorption form, the two Br atoms are initially attached to the on-top and to one of the edge Pt atoms. However, the geometry optimization leads to the structure shown in Figure 4c where one of the Br atoms makes in-plane symmetric two bonds with the two nearest edge Pt atoms. Its overall adsorption energy amounts to 72.9 kcal/mol as compared to the isolated noninteracting Pt_{10} cluster

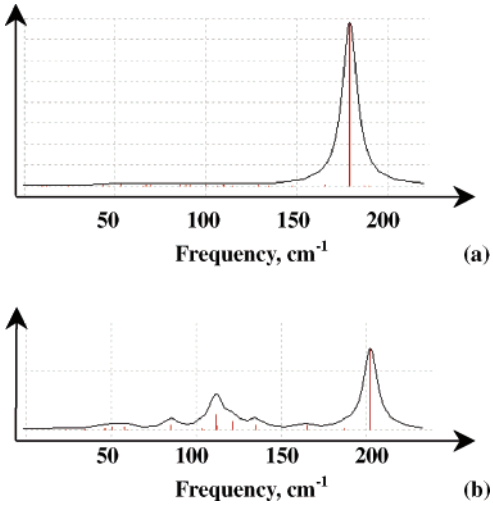

Figure 5. Theoretical IR spectra of bromine adsorbed on the Pt(111) surface: (a) molecular Br_2 adsorption and (b) atomic Br adsorption.

and the Br_2 molecule. Interesting to note is that both molecular and dissociative adsorption of Br_2 did not alter the optimal spin state of the bare Pt_{10} cluster, while an atomic Br adsorption lowers it, as is found before in the case of the on-top adsorption of NO. Based on these energetic criteria we conclude that the STM tip immersed into a bromine solution may contain only dissociated bromine atoms that are strongly bound with the surface Pt atoms. This finding is in complete agreement with the results of experimental investigations.[15,17] As a result, one may not see the ν_{BrBr} stretching vibration of the adsorbed Br_2 molecule (see Figure 5a) because it will be blue shifted due to the appearance of the ν_{PtBr} stretching vibration centered at around 202 cm^{-1} (see Figure 5b). Note that the theoretical IR spectrum has been simulated by the Lorentzian broadening of the calculated discrete vibrations with a half width of 20 cm^{-1}.

Summary and Conclusions

The obtained results of the density functional calculations at the B3LYP level using the above combined basis sets can be concluded as follows:

1. The adsorption energies of NO on different sites of the Pt(111) surface lie in close proximity to each other, while the relative stability order of adsorption complexes can be expressed as on-top > fcc ≈ hcp that correlates directly with the HOMO level. At low NO coverage, the first peak is predicted to appear at around 1515 cm^{-1}, while it would shift to 1707 cm^{-1} at high NO coverage in accordance with experimental observations.

2. An atomic Br as well as the dissociative adsorption of Br_2 proceed highly favorably as compared to the molecular adsorption of Br_2 on the top position of the Pt(111) surface that is the least favorable one. Both the molecular and dissociative adsorption of Br_2 did not alter the optimal spin state of the bare Pt_{10} cluster, while an atomic Br adsorption lowers it for one.

3. The STM tip immersed into a bromine solution may contain only dissociated bromine atoms that strongly bind with the surface Pt atoms. As a result, the ν_{BrBr} stretching

vibration of the adsorbed Br_2 molecule cannot be seen because of a blue shift and are centered at ca. 202 cm^{-1}.

Acknowledgment. We gratefully acknowledge supercomputing resources provided by the Information Synergy Center of Tohoku University. The present work was supported by a Grant-in-Aid from the Ministry of Education, Science, and Culture of Japan (16072203).

References

(1) (a) Schmatloch, V.; Kruse, N. *Surf. Sci.* **1992**, *270*, 488−494. (b) Gland, J. L.; Sexton, B. A. *Surf. Sci.* **1980**, *94*, 355−368. (c) Hayden, B. F. *Surf. Sci*. **1983**, *131*, 419−432.

(2) (a) Hammer, B. J. *J. Catal.* **2001**, *199*, 171−176. (b) Hammer, B. *Phys. Rev. Lett*. **1999**, *83*, 3681−3684. (c) Hammer, B.; Norskov, J. K. *Phys. Rev. Lett*. **1997**, *79*, 4441−4444.

(3) Aizawa, H.; Morikawa, Y.; Tsuneyuki, S.; Fukutani, K.; Ohno, T. *Surf. Sci.* **2002**, *514*, 394−403.

(4) Burch, R.; Daniells, S. T.; Hu, P. *J. Chem. Phys*. **2002**, *117*, 2902−2908.

(5) Esch, F.; Greber, T.; Kennou, S.; Siokou, A.; Ladas, S.; Imbihl, R. *Catal. Lett*. **1996**, *38*, 165−170.

(6) Nakatsuji, H.; Matsumune, N.; Kuramoto, K. *J. Chem. Theory Comput*. **2005**, *1*, 239−247.

(7) Tang, H.; Trout, B. L. *J. Phys. Chem. B* **2005**, *109*, 17630−17634.

(8) Brown, W. A.; King D. A. *J. Phys. Chem. B* **2000**, *104*, 2578−2595.

(9) Ge, Q.; King, D. A. *Chem. Phys. Lett*. **1998**, *285*, 15−20.

(10) Koper, M. T. M.; van Santen, R. A.; Wasilevski, S. A.; Weaver, M. J. *J. Chem. Phys*. **2000**, *113*, 4392−4407.

(11) Shelef, M.; Graham, G. W. *Catal. Rev. Sci.. Eng.* **1994**, *36*, 433−457.

(12) Taylor, K. C. *Catal. Rev. Sci. Eng.* **1993**, *35*, 457−481.

(13) Shelef, M. *Chem. Rev.* **1995**, *95*, 209−225.

(14) Zhanpeisov, N. U.; Higashimoto, S.; Anpo, M. *Int. J. Quantum Chem*. **2001**, *84*, 677−685.

(15) Ferro, S.; de Battisti, A. *J. Appl. Electrochem*. **2004**, *34*, 981−987.

(16) Swamy, K.; Hanesch, P.; Sandl, P.; Bertel, E. *Surf. Sci*. **2000**, *466*, 11−29.

(17) Xu, H.; Harrison, I. *J. Phys. Chem. B* **1999**, *103*, 11233−11236.

(18) Orts, J. M.; Gomez, R.; Feliu. *J. Electroanal. Chem*. **1999**, *467*, 11−19.

(19) Solomon, T.; Wieckowski, A.; Rosasco, S. D.; Hubbard, A. T. *Surf. Sci*. **1984**, *147*, 241−251.

(20) Bittner, A. M.; Wintterlin, J.; Beran, B.; Ertl, G. *Surf. Sci*. **1995**, *335*, 291−299.

(21) (a) Binnig, G.; Rohrer, H.; Gerber, Ch.; Weibel, E. *Phys. Rev. Lett*. **1982**, *49*, 57−61. (b) Binnig, G.; Rohrer, H. *Rev. Mod. Phys*. **1987**, *59*, 615−625.

(22) (a) van Hove, M. A.; Cerda, J.; Sautet, P.; Bocquet, M. L.; Salmeron, M. *Prog. Surf. Sci*. **1997**, *54*, 315−329. (b) Bocquet, M. L.; Cerda, J.; Sautet, P. *Phys. Rev. B* **1999**, *59*, 15437−15445. (c) Sautet, P. *Chem. Rev.* **1997**, *97*, 1097−1116; (d) Carlisle, C. I.; King, D. A.; Bocquet, M. L.; Cerda, J.; Sautet, P. *Phys. Rev. Lett*. **2000**, *84*, 3899−3902.

(23) Hofer, W. A.; Foster, A. S.; Schluger, A. L. *Rev. Mod. Phys*. **2003**, *75*, 1287−1332.

(24) Drakova, D. *Rep. Prog. Phys*. **2001**, *64*, 205−290.

(25) Frisch, M. J.; Trucks, G. W.; Schlegel, H. B.; Scuseria, G. E.; Robb, M. A.; Cheeseman, J. R.; Montgomery, J. A., Jr.; Vreven, T.; Kudin, K. N.; Burant, J. C.; Millam, J. M.; Iyengar, S. S.; Tomasi, J.; Barone, V.; Mennucci, B.; Cossi, M.; Scalmani, G.; Rega, N.; Petersson, G. A.; Nakatsuji, H.; Hada, M.; Ehara, M.; Toyota, K.; Fukuda, R.; Hasegawa, J.; Ishida, M.; Nakajima, T.; Honda, Y.; Kitao, O.; Nakai, H.; Klene, M.; Li, X.; Knox, J. E.; Hratchian, H. P.; Cross, J. B.; Bakken, V.; Adamo, C.; Jaramillo, J.; Gomperts, R.; Stratmann, R. E.; Yazyev, O.; Austin, A. J.; Cammi, R.; Pomelli, C.; Ochterski, J. W.; Ayala, P. Y.; Morokuma, K.; Voth, G. A.; Salvador, P.; Dannenberg, J. J.; Zakrzewski, V. G.; Dapprich, S.; Daniels, A. D.; Strain, M. C.; Farkas, O.; Malick, D. K.; Rabuck, A.; Raghavachari, K.; Foresman, J. B.; Ortiz, J. V.; Cui, Q.; Baboul, A. G.; Clifford, S.; Cioslowski, J.; Stefanov, B. B.; Liu, G.; Liashenko, A.; Piskorz, P.; Komaromi, I.; Martin, R. L.; Fox, D. J.; Keith, T.; Al-Laham, M. A.; Peng, C. Y.; Nanayakkara, A.; Challacombe, M.; Gill, P. M. W.; Johnson, B.; Chen, W.; Wong, M. W.; Gonzalez, C.; Pople, J. A. *Gaussian 03, Revision C.02*; Gaussian, Inc.: Wallingford, CT, 2004.

(26) (a) Becke, A. D. *Phys. Rev. A* **1988**, *38*, 3098−3100. (b) Lee, C.; Yang, W.; Parr, R. G. *Phys. Rev. B* **1988**, *37*, 785−789.

(27) Matsumoto, M.; Tatsumi, N.; Fukutani, K.; Okano, T. *Surf. Sci*. **2002**, *513*, 485−500.

(28) Hansen, K. H.; Sljivancanin, Z.; Hammer, B.; Laegsgaard, E.; Besenbacher, F.; Stensgaard, I. *Surf. Sci*. **2002**, *496*, 1−9.

(29) Materer, N.; Barbieri, A.; Gardin, D.; Starke, U.; Batteas, J. D.; Vanhove, M. A.; Somorjai, G. A. *Surf. Sci*. **1994**, *303*, 319−332.

(30) Because of evident facts originating from either the incomplete treatment of electroncorrelation or neglect of mechanical anharmonicity or basis set truncation effects, the calculated harmonic frequencies are generally overestimated.[31,32] The B3LYP method overestimates also the calculated harmonic frequencies, and, for this reason, the scaling factors have been proposed in the literature.[32,33]

(31) Scott, A. P.; Radom, L. *J. Phys. Chem*. **1996**, *100*, 16502−16513.

(32) (a) Halls, M. D.; Velkovski, J.; Schlegel, H. B. *Theor. Chem. Acc*. **2001**, *105*, 413−421. (b) Halls, M. D.; Raghavachari, K. *J. Phys. Chem. B* **2004**, *108*, 19388−19391.

(33) (a) Zhanpeisov, N. U.; Martra, G.; Ju, W. S.; Matsuoka, M.; Coluccia, S.; Anpo, M. *J. Mol. Catal. A: Chem.* **2003**, *201*, 237−246. (b) Zhanpeisov, N. U.; Nishio, S.; Fukumura, H. *Int. J. Quantum Chem.* **2005**, *105*, 368−375.

CT050308M